

Voltage preservation in Intermediate Band Solar Cells

Daniel Suchet^{*1,2}, Amaury Delamarre^{1,2}, Nicolas Cavassilas^{2,3}, Zacharie Jehl^{1,2}, Yoshitaka Okada^{1,2}, Masakazu Sugiyama^{1,2}, and Jean-Francois Guillemoles^{1,4}

¹Research Center for Advanced Science and Technology, The University of Tokyo, 4-6-1 Komaba, Meguro-ku, Tokyo 153-8904, Japan

²LIA NextPV, Research Center for Advanced Science and Technology, The University of Tokyo, 4-6-1 Komaba, Meguro-ku, Tokyo 153-8904, Japan

³Aix Marseille Université, CNRS, Université de Toulon, IM2NP UMR 7334, 13397, Marseille, France

⁴Institut Photovoltaïque d'Ile de France (IPVF), UMR 9006, 30 route départementale 128, 91120, Palaiseau, France

October 5, 2018

Abstract

Intermediate Band Solar Cell is an advanced concept for solar energy conversion in which two low-energy photons can promote an electron to the conduction band through a so-called *intermediate band*. To limit recombination and preserve the photo-generated voltage, generation to- and from the intermediate band should be matched. However, all practical realizations experienced a significant voltage degradation as compared to a single junction without intermediate band. In this work, we develop a novel analytical optimization method based on Lagrange multipliers. We demonstrate that an Intermediate Band Solar Cell under solar spectrum cannot meet voltage preservation and current matching at the same time. By contrast, we show that the implementation of an energy shift (*electronic ratchet*) in any of the bands allows those two criteria to be filled simultaneously. Additional insights are provided by the numerical study of the short circuit current and fill factor of the systems at stake, which show that a system with ratchet benefits from the same current increase as a standard Intermediate Band Solar Cell (same short-circuit current), while maintaining I-V properties of a single junction (same open-voltage circuit, same fill factor).

1 Introduction

Intermediate band solar cells were introduced as a new concept of photovoltaic converter to overcome the celebrated Shockley Queisser limit [1]. IBSC aims at collecting some photons with energy below the energy bandgap, that would not be absorbed in a standard single-junction solar cell. To do so, a so-called intermediate band is introduced within the bandgap and serves as built-in up-converter, allowing two photons transitions from the valence band to the intermediate band (IV transition) and from the intermediate band to the conduction band (IC transition). This additional absorption increases the current produced

by the device, and allows theoretically for an efficiency enhancement from 31% to 47% under one sun illumination [2].

IBSC have received large attention over the last decades, and several refinement have been brought to the seminal concept [3, 4, 5, 6]. However, despite experimental efforts (see [7] and references therein), no fully working proof of concept has been reported yet. One of the main blocking point is certainly the voltage degradation induced by recombination through the intermediate band [8]. Furthermore, it was recently suggested that the combined effect of small non-idealities, such as narrow absorption and non radiative recombination on the IC transition could pre-

*Email daniel.suchet@polytechnique.org

vent IBSC from reaching SQ limit [9]. An elegant way to circumvent this issue is to introduce an *electronic ratchet*, i.e. an energy shift between the IV and IC transitions [10]. Possible realizations could rely on succession of quantum wells organized with tailored width [9] or as a quantum cascade [11], on 2D materials [12] or on compounds with transition metal [13]. It has been shown numerically that such *electronic ratchet* not only increases the conversion efficiency of IBSC, but also strongly enhances their resilience against the aforementioned non-idealities. Despite the increasing interest for the ratchet feature [14], the physics at stake behind the ratchet system is not trivial [15, 16], and received little attention so far.

While conversion efficiency is a well suited indicator for practical purposes of energy conversion, it is a too aggregated figure of merit to provide a clear picture of the conversion processes. This is especially true for complex systems such as IBSC, where many processes take place at the same time [10]. On the other hand, electrical properties of the device, such as open circuit voltage, short circuit current and fill factor, offer a deeper perspective. Most notably, being directly related to the carriers free energy, open circuit voltage has been proven to bring insight on the system thermodynamics [17], and can be used to estimate the entropy production occurring during the photon-to-carrier conversion [18]. Studying open-circuit voltage also sheds light on the voltage preservation issue that prevents standard IBSC from exceeding the Shockley Queisser limit.

In this work, we study the open circuit voltage of a IBSC with electronic ratchet (RBSC). Our approach relies on Lagrange multipliers, which allows to estimate the optimal configuration of a system under constraints. Using this powerful technique, we show analytically that an optimal RBSC displays the same V_{OC} as a single junction with the same energy gap. This property can be used to estimate the optimal band configuration. By contrast, we show that IBSC can not preserve voltage and ensure a good current matching at the same time. Finally, complementary figures of merit are numerically studied, suggesting physical interpretation of the ratchet influence.

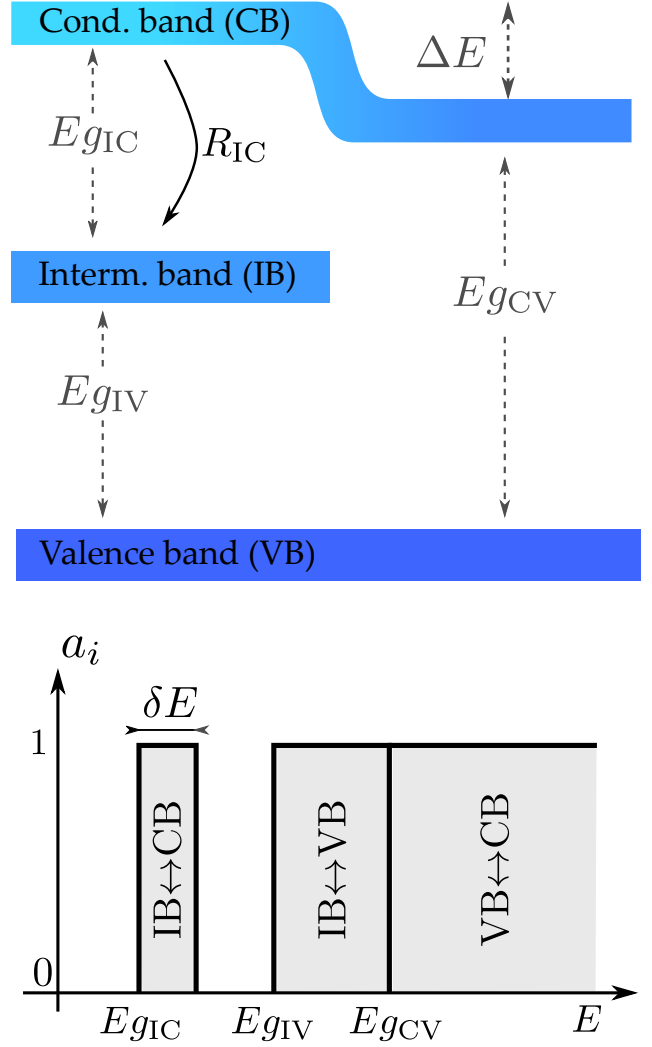


Figure 1: Band configuration and absorptivity in a RBSC. In the non-overlapping absorption model, photons with between $E_{g_{IC}}$ and $E_{g_{IC}} + \delta E$ are absorbed and emitted in the intermediate to conduction (IC) transition ; those with energy between $E_{g_{IV}}$ and $E_{g_{CV}}$ in the IV transition and those with energy above $E_{g_{CV}}$ in the CV transition. Non radiative losses are considered on the IC transitions, in addition to radiative recombinations. We account for this effect through a radiative efficiency factor increasing R_{IC} (pictured with a curved arrow).

2 Model and notations

We will use the detailed balance model introduced and detailed by Yoshida *et al.* [10], with notations presented in Fig 1. The carrier generation G_i and radiative recombination R_i rates for each transition i are

given by a generalized Planck's law [17]

$$G_i = \frac{f}{4\pi^3 \hbar^3 c^2} \int_0^\infty dE \frac{a_i(E) E^2}{\exp\left(\frac{E}{kT_S}\right) - 1} \quad (1)$$

$$R_i = \frac{1}{r_{\text{rad},i}} \frac{1}{4\pi^2 \hbar^3 c^2} \int_0^\infty dE \frac{\epsilon_i(E) E^2}{\exp\left(\frac{E - \Delta\mu_i}{kT_C}\right) - 1} \quad (2)$$

where $i = VC, IV, IC$ labels the valence to conduction, valence to intermediate and intermediate to conduction band transitions respectively. f is a geometrical concentration factor, equal to 6.79×10^{-5} for an un-concentrated illumination. The temperature T is taken to $T_S = 6000$ K for generation rates (dark current is neglected) and $T_C = 300$ K for recombination rates, while the quasi Fermi level splitting $\Delta\mu_i$ are all zero for the solar black-body radiation. To ease notations, we will note $\Delta\tilde{\mu}_i = \Delta\mu_i/kT_C$. The absorptivity, emissivity and radiative efficiency of each transition are denoted $a_i(E)$, $\epsilon_i(E)$ and $r_{\text{rad},i}$ respectively. Owing to the Kirchhoff's law of radiation, emissivity is equal to absorptivity for each wavelength, and both generation and recombination rates can be inferred from a_i only. Following previous models, we will consider non-overlapping perfect absorptivity ($a_i(E) = 1$) and radiative limit ($r_{\text{rad},i} = 1$) for VC and IV transitions, while the IC transition is considered with a narrow span δE and includes non-radiative recombination (see Fig. 1). This approach accounts for constraints raised by the use of nanostructures for IBSC, where the IB - CB transition is intra-band [9, 19].

The energy shift of the electronic ratchet is defined as

$$E_{gIV} + E_{gIC} = E_{gCV} + \Delta E. \quad (3)$$

Note that the ratchet shift can be indifferently considered on the conduction band (as is the case here) or on the intermediate band [15]. In the following, we will refer to systems with finite ΔE as Ratchet Band Solar Cells (RBSC) and systems with $\Delta E = 0$ as IBSC - even though both systems rely on electronic transition through an intermediate band.

Electrically, these systems are equivalent to two diodes connected in series (IC and IV transitions), in parallel to a third diode (CV transition). As clear from this picture, Kirchhoff's voltage and current laws impose constraints on the system, and can be written as

$$qV = \Delta\mu_{CV} = \Delta\mu_{IV} + \Delta\mu_{IC} \quad (4)$$

$$G_{IV} - R_{IV} = G_{IC} - R_{IC} \quad (5)$$

To simplify calculations, we will consider the Boltz-

mann approximation of the recombination rates

$$R_i \simeq R_i^0 \exp\left(\frac{\Delta\mu_i}{kT_C}\right) \quad (6)$$

which is valid for all gaps both at open circuit voltage V_{OC} and maximum power point V_m under un-concentrated illumination.

In the following, we will often consider the *best-gap voltage* $V_{gm,i}$, defined as the bias for which an isolated junction with an energy gap E_{g_i} would be optimal

$$\partial_{E_{g_i}} [V (G_i - R_i(V))] \Big|_{V=V_{gm,i}} = 0 \quad (7)$$

The best-gap voltage is determined by the absorptivity, and thus depends only on the energy gap and absorption width. Within Boltzmann approximation (6), $V_{gm,i}$ can be expressed as:

$$\exp\left(\frac{qV_{gm,i}(E_{g_i}, \delta E)}{kT_C}\right) \simeq \frac{\partial_{E_{g_i}} G_i \Big|_{E_{g_i}=E_{g_i}}}{\partial_{E_{g_i}} R_i^0 \Big|_{E_{g_i}=E_{g_i}}}. \quad (8)$$

The best-gap voltage should not be confused with the maximum power point V_m , defined for a given absorptivity as

$$\partial_V [V (G - R(V))] \Big|_{V=V_m} = 0 \quad (9)$$

Considered at any value of the energy gap, the best-gap voltage is *a priori* different from the maximum power point, and both quantities coincide only for the optimal configuration. However, for a single junction, the best-voltage gap has been proven to be numerically close to the maximum power point down to few percents [20], and we will therefore consider

$$V_{gm,CV} \simeq V_m^{(1)} \quad (10)$$

where $V_m^{(1)}$ is the maximal power point of a single junction with gap E_{gCV} .

3 Voltage preservation in RBSC

Following the model presented in the previous section, the efficiency of RBSC system can be estimated from six parameters $\{E_{g_i}, \Delta\mu_i\}$, submitted to two constraints eq. (4) and (5). In this section, we will study the open circuit voltage of an optimal RBSC, ie for a configuration such that the power output power of the cell

$$P(E_{g_i}, \Delta\mu_i) = \sum_i \Delta\mu_i \left(G_i - R_i^0 e^{\Delta\tilde{\mu}_i} \right) \quad (11)$$

is maximum. An appropriate framework to account for such a system is provided by Lagrange multiplier [21], where all parameters are treated as independent, and constraints are included explicitly in the Lagrangian

$$L_R = P + \lambda_J [(G_{IV} - R_{IV}) - (G_{IC} - R_{IC})] + \lambda_V [\Delta\mu_{CV} - (\Delta\mu_{IV} + \Delta\mu_{IC})] \quad (12)$$

Note that this approach can be extended to standard IBSC by adding a constraint on the energy gaps

$$L_{IBSC} = L_R + \lambda_E [E_{g_{CV}} - (E_{g_{IV}} + E_{g_{IC}})] \quad (13)$$

which suggests that the benefit of the electronic ratchet comes from the relaxation of this additional constraint.

The optimal configuration for the RBSC is reached when derivatives of the Lagrangian (12) with respect to the system parameters $\{E_{g_i}, \Delta\mu_i\}$ and Lagrange multipliers $\{\lambda_J, \lambda_V\}$ are all equal to zero. The detailed calculations are presented in annex, and provide relations between parameters in optimal configuration.

It is notably possible to express the maximum power point of an optimal RBSC $V_m = \Delta\mu_{CV}/q$ as a function of the three energy gaps only

$$\exp\left(\frac{qV_m}{kT_C}\right) = \exp\left(\frac{qV_{gm,CV}}{kT_C}\right) \left(1 + \frac{R_{IC}^0 e^{\frac{qV_{gm,IC}}{kT_C}} - 1}{R_{IV}^0 e^{\frac{qV_{gm,IV}}{kT_C}}}\right) \quad (14)$$

The right hand side denominator can be shown to be close to unity. Indeed, to optimize current matching through the intermediate band and limit recombination, generation rates G_{IC} and G_{IV} should be equal (see section 4). However, a too narrow absorption width δE can prevent G_{IC} from reaching values close to G_{IV} . In any case, G_{IV} forms an upper bound for the optimal value of G_{IC} . Due to current conservation eq.(4), R_{IC} is therefore also limited by R_{IV} , and is much smaller than this upper bound for narrow transitions. We will thus consider

$$R_{IC}^0 e^{\frac{qV_{gm,IC}}{kT_C}} \leq R_{IV}^0 e^{\frac{qV_{gm,IV}}{kT_C}} \quad (15)$$

With an estimation error smaller than $\log 2 kT_C/q$ (less than 2% of relative value), the previous expression can be simplified to

$$V_m \simeq V_{gm,CV} \simeq V_m^{(1)} \quad (16)$$

where the last equality follows from eq. (10). The maximum power point for a RBSC is close to that of single junction with the same large gap $E_{g_{CV}}$.

Furthermore, it can also be shown (see Appendix) that the open circuit voltage V_{OC} and maximum power point V_m for a RBSC are related by the exact same relation as for a single junction:

$$\left(1 + \frac{qV_m}{kT}\right) \exp\left(\frac{qV_m}{kT_C}\right) = \exp\left(\frac{qV_{OC}}{kT_C}\right) \quad (17)$$

As this relation is monotonous for positive biases, equation (16) implies the equality of open circuit voltage between the optimal RBSC and the corresponding single junction with the same large gap:

$$V_{OC} \simeq V_{OC}^{(1)} \quad (18)$$

This proves approximate voltage preservation in an optimal RBSC. This remarkable result also implies that, in an optimal RBSC, all three transitions reach their respective open-circuit condition $G_i = R_i$ simultaneously.

The open-circuit voltages of RBSC and IBSC are compared to that of a single junction sharing the same gap $E_{g_{CV}}$ on Fig. 2. For illustration purpose, we have taken an absorption width $\delta E = 150$ meV [22] and a radiative efficiency $r_{rad,IC}$ equal to 1 or 10^{-3} [23]. For small $E_{g_{CV}}$, an IBSC is limited to Shockley Queisser limit. No current flows through the intermediate transition, and the IBSC behaves like a single junction. At larger gaps, the intermediate transition contributes to the current, increasing the system efficiency. However, this transition also results in a loss larger than 10% of the open circuit voltage as compared to the single junction. By contrast, the open-circuit voltage RBSC remains very close to $V_{OC}^{(1)}$ (less than 1%), regardless of the main gap or radiative efficiency considered.

It should also be noted that, due to the Lagrange multiplier approach used for its derivation, voltage preservation (18) is only valid for optimal set of parameters $\{E_{g_i}, \Delta\mu_i\}$. However, its numerical validity range appears to be significantly larger, and holds for a large span of gaps $E_{g_{CV}}$. Therefore, RBSC are expected to exhibit voltage preservation even in non-optimal situations.

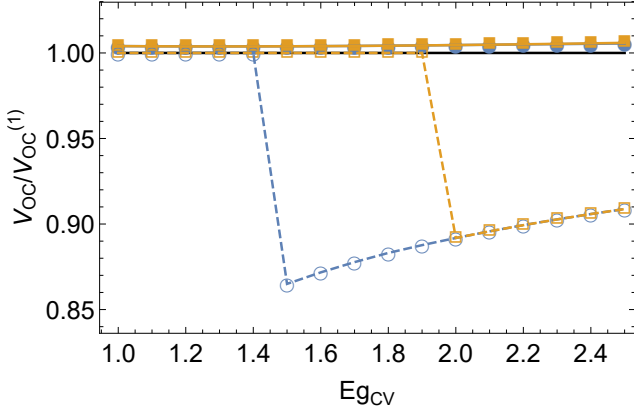


Figure 2: Open circuit voltage of RBSC (plain line and filled symbols) and IBSC (dashed line and empty symbols), normalized to that of a single junction with the same main gap $E_{g_{CV}}$. Absorption width is taken to $\delta E = 150$ meV and $r_{rad,IC}$ to 1 (blue circles) and 10^{-3} (yellow square). For each gap $E_{g_{CV}}$, the band configuration of both structures are determined by optimizing the conversion efficiency.

4 Optimization criteria for RBSC

In previous works, RBSC band configuration was optimized numerically by testing all possible combinations of parameters matching Kirchhoff laws eq.(4) and (5). This brute force method can be time consuming, but requires no physical understanding of the system. The Lagrange multiplier approach presented in the previous section provides additional constraints (see eq.(14) and eq.(33-34) in annex), reducing the parameter space. A sixth expression can be derived from the Lagrangian L_R , providing a closure relation on the electrical current J_m at the maximum power point:

$$\frac{J_m}{q} = \frac{qV_m}{kT_C} \exp\left(\frac{qV_m}{kT_C}\right) \times \left(R_{CV}^0 + \frac{R_{IV}^0 R_{IC}^0}{R_{IC}^0 e^{\frac{qV_{gm,IC}}{kT_C}} + R_{IV}^0 e^{\frac{qV_{gm,IV}}{kT_C}}} \right) \quad (19)$$

These relations can be used to estimate the optimal set of bandgaps and operating voltages. However, it is also insightful to estimate the optimal bandgap configuration $\{E_{g_i}\}$ alone, by considering only generation rates which are independent of the applied voltage.

A first criteria was suggested in [10] that, to favor current matching in the intermediate transitions, and thus minimize radiative losses, generation rates should verify $G_{IC} = G_{IV}$. In the general case of a narrow absorption considered in this work, this criteria cannot always be met and the current matching

criteria should rather be expressed by minimizing the quantity

$$|G_{IC} - G_{IV}| \quad (20)$$

Furthermore, the voltage preservation relation eq. (18) can be expressed in terms of generation and recombination rates (see appendix) as:

$$\frac{G_{IV}G_{IC}}{R_{IV}^0 R_{IC}^0} = \frac{G_{CV}}{R_{CV}^0} \quad (21)$$

Since these two criteria only depend on the energy gaps, the optimal values of $E_{g_{IV}}$ and $E_{g_{IC}}$ can be determined if the optimal value of $E_{g_{CV}}$ is known. The efficiency of the structure calculated from these criteria is compared to the efficiency estimated from brute force optimization on Figure 3. Several conclusions can be reached.

First, despite being approximate relations, the two criteria eq.(20 - 21) presented here allow to recovers extremely well the values of the brute force method. This agreement shows that most of the physics of the RBSC is contained in current matching and voltage preservation.

Second, as for voltage preservation, the validity of these criteria extends on a large range around the global optimal, allowing for the estimation of the optimal ratchet band structure $\{E_{g_{IV}}, E_{g_{IC}}\}$ for any gap $E_{g_{CV}}$ of practical use.

Third, these numerical calculations show that, for both criteria to be met simultaneously, a non-zero ratchet shift ΔE must be considered. An important corollary of this result is therefore that a standard IBSC without electronic ratchet can not satisfy current matching and voltage preservation at the same time under un-concentrated light.

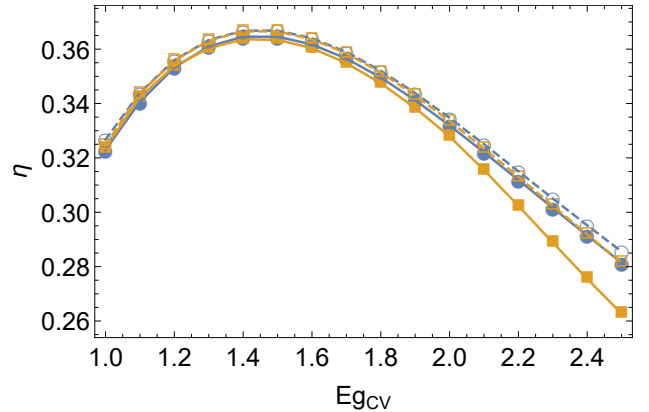


Figure 3: Conversion efficiency as estimate by the brute force method (dashed line and empty symbols) and from criteria eq.(20-21) (plain line and filled symbols). Absorption width is taken to $\delta E = 150$ meV and $r_{rad,IC}$ to 1 (blue circles) and 10^{-3} (yellow square).

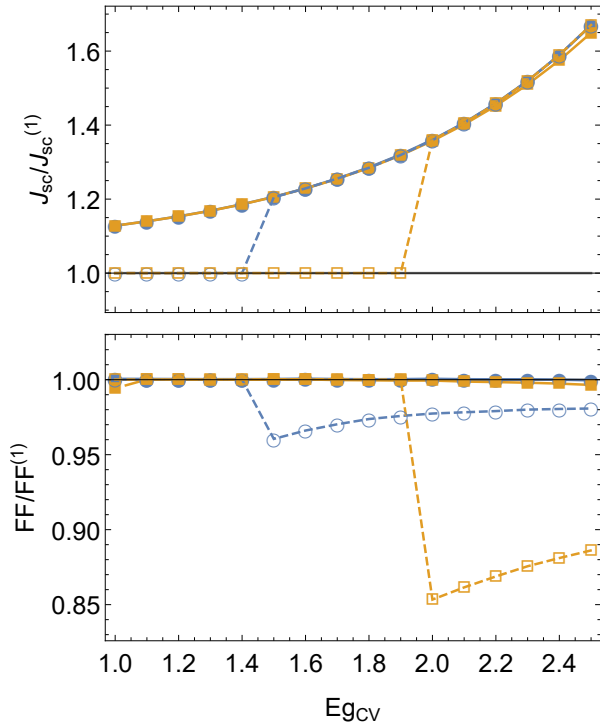


Figure 4: Short circuit current (above) and Fill Factor (below) of RBSC (plain line and filled symbols) and IBSC (dashed line and empty symbols), normalized to that of a single junction with the same main gap E_{gCV} . Absorption width is taken to $\delta E = 150$ meV and $r_{rad,IC}$ to 1 (blue circles) and 10^{-3} (yellow square). For each gap E_{gCV} , the band configuration of both structures are determined by optimizing the conversion efficiency. As noted in previous works [9], unlike for standard IBSC, the efficiency of a RBSC is marginally affected by non-radiative losses.

5 The best of both worlds

Finally, as a qualitative extension to the previous study, we estimate numerically complementary figures of merit. Figure 4 compares compares the short circuit current J_{sc} and the fill factor FF reached by an optimal RBSC, IBSC and single junction sharing the same large E_{gCV} .

As in Fig. 2, the IBSC works as a single junction for small gaps. The intermediate transition contribution appears as a significant increase in the short circuit current, but is accompanied by a decrease of the fill factor (in addition to the voltage loss mentioned above). When non radiative losses are considered, the trade-off between the beneficial and detrimental effects of the intermediate transition prevent the system from exceeding the Shockley-Queisser limit [9].

By contrast, the RBSC maintains also a fill factor very close to that of a single junction, regardless of the main gap or radiative efficiency considered, and bene-

fits from the same current increase as an optimal IBSC. In perspective of voltage preservation demonstrated above, it thus appears that the electronic ratchet enables RBSC to benefit from the best of two worlds, and to take advantage of the best characteristics in both IBSC and single junction systems.

6 Conclusions

In summary, we have studied theoretically electrical properties of intermediate band solar cells featuring an electronic ratchet. We have shown numerically that RBSC can reach the same open circuit voltage and fill factor as a single junction with the same gap, while benefiting from the same current increase as a standard IBSC without ratchet. To investigate the underlying physics, we have proven that the optimal RBSC is characterized by voltage preservation and current matching between IC and IV transitions. By contrast, an IBSC without ratchet is unable to meet both criteria simultaneously and the resulting trade-off limits its conversion efficiency. This analytical result has been obtained using Lagrange multipliers, a method particularly well suited for optimization under constraints and which will certainly bring new insights on many problems in photovoltaics.

Acknowledgments

DS and NC thank the Japan Society for the Promotion of Science (JSPS) for financial support (grant number PE16763).

References

- [1] W. Shockley and H. J. Queisser, "Detailed balance limit of efficiency of p-n junction solar cells," *Journal of Applied Physics*, vol. 32, no. 3, pp. 510–519, 1961.
- [2] A. Luque and A. Marti, "Increasing the efficiency of ideal solar cells by photon induced transitions at intermediate levels," *Physical Review Letters*, vol. 78, no. 26, p. 5014, 1997.
- [3] A. Luque, A. Marti, and L. Cuadra, "Thermodynamic consistency of sub-bandgap absorbing solar cell proposals," *IEEE Transactions on Electron Devices*, vol. 48, no. 9, pp. 2118–2124, 2001.

- [4] L. Cuadra, A. Marti, and A. Luque, "Influence of the overlap between the absorption coefficients on the efficiency of the intermediate band solar cell," *IEEE Transactions on Electron Devices*, vol. 51, no. 6, pp. 1002–1007, 2004.
- [5] M. Y. Levy and C. Honsberg, "Solar cell with an intermediate band of finite width," *Physical Review B*, vol. 78, no. 16, 2008.
- [6] M. Y. Levy and C. Honsberg, "Intraband absorption in solar cells with an intermediate band," *Journal of Applied Physics*, vol. 104, no. 11, p. 113103, 2008.
- [7] Y. Okada, N. J. Ekins-Daukes, T. Kita, R. Tamaki, M. Yoshida, A. Pusch, O. Hess, C. C. Phillips, D. J. Farrell, K. Yoshida, N. Ahsan, Y. Shoji, T. Sogabe, and J.-F. Guillemoles, "Intermediate band solar cells: Recent progress and future directions," *Applied Physics Reviews*, vol. 2, no. 2, p. 021302, 2015.
- [8] P. G. Linares, A. Marti, E. Antolin, C. D. Farmer, I. Ramiro, C. R. Stanley, and A. Luque, "Voltage recovery in intermediate band solar cells," *Solar Energy Materials and Solar Cells*, vol. 98, pp. 240–244, 2012.
- [9] A. Delamarre, D. Suchet, N. Cavassilas, Y. Okada, M. Sugiyama, and J.-F. Guillemoles, "An electronic ratchet is required in nanostructured intermediate band solar cells," *Submitted to IEEE JPV*, 2018.
- [10] M. Yoshida, N. J. Ekins-Daukes, D. J. Farrell, and C. C. Phillips, "Photon ratchet intermediate band solar cells," *Applied Physics Letters*, vol. 100, no. 26, p. 263902, 2012.
- [11] O. J. Curtin, M. Yoshida, A. Pusch, N. P. Hylton, N. J. Ekins-Daukes, C. C. Phillips, and O. Hess, "Quantum cascade photon ratchets for intermediate-band solar cells," *IEEE Journal of Photovoltaics*, vol. 6, no. 3, pp. 673–678, 2016.
- [12] S.-F. Chen and Y.-R. Wu, "A design of intermediate band solar cell for photon ratchet with multilayer MoS₂ nanoribbons," *Applied Physics Letters*, vol. 110, p. 201109, May 2017.
- [13] P. Olsson, C. Domain, and J.-F. Guillemoles, "Ferromagnetic Compounds for High Efficiency Photovoltaic Conversion: The Case of AlP:Cr," *Physical Review Letters*, vol. 102, June 2009.
- [14] G. Sahoo and G. Mishra, "Use of ratchet band in a quantum dot embedded intermediate band solar cell to enrich the photo response," *Materials Letters*, Jan. 2018.
- [15] A. Pusch, M. Yoshida, N. P. Hylton, A. Mellor, C. C. Phillips, O. Hess, and N. J. Ekins-Daukes, "Limiting efficiencies for intermediate band solar cells with partial absorptivity: the case for a quantum ratchet: Limiting efficiencies for intermediate band solar cells," *Progress in Photovoltaics: Research and Applications*, vol. 24, no. 5, pp. 656–662, 2016.
- [16] A. T. Bezerra and N. Studart, "Lifetime enhancement for multiphoton absorption in intermediate band solar cells," *Journal of Physics D: Applied Physics*, vol. 50, p. 305501, Aug. 2017.
- [17] P. Wurfel, "The chemical potential of radiation," *Journal of Physics C: Solid State Physics*, vol. 15, no. 18, pp. 3967–3985, 1982.
- [18] T. Markvart, "Thermodynamics of losses in photovoltaic conversion," *Applied Physics Letters*, vol. 91, no. 6, p. 064102, 2007.
- [19] N. Cavassilas, D. Suchet, A. Delamarre, F. Michelini, M. Bescond, Y. Okada, M. Sugiyama, and J.-F. Guillemoles, "Beneficial impact of tunneling in nano-structured intermediate-band solar cell," *Submitted to IEEE JPV, arXiv ID: 1802.04212*, 2018.
- [20] L. C. Hirst and N. J. Ekins-Daukes, "Fundamental losses in solar cells," *Progress in Photovoltaics: Research and Applications*, vol. 19, no. 3, pp. 286–293, 2011.
- [21] H. Goldstein, C. P. Poole, and J. L. Safko, *Classical mechanics*. San Francisco, NJ: Addison Wesley, 3. ed ed., 2002. OCLC: 248389949.
- [22] N. Georgiev, T. Dekorsy, F. Eichhorn, M. Helm, M. P. Semtsiv, and W. T. Masselink, "Short-wavelength intersubband absorption in strain compensated InGaAs/AlAs quantum well structures grown on InP," *Applied Physics Letters*, vol. 83, pp. 210–212, July 2003.
- [23] R. Q. Yang, "Infrared laser based on intersubband transitions in quantum wells," *Superlattices and Microstructures*, vol. 17, pp. 77–83, Jan. 1995.

Appendix

Open-circuit voltage and Maximum power point in IBSC

In this section, we demonstrate eq.(17) and (21) used in the main text from the I-V behavior of an IBSC (with or without ratchet). To estimate this behavior, we express the current flowing at a bias $qV = \Delta\mu_{CV}$ as the sum of the direct and intermediate contributions

$$\frac{J}{q} = \left(G_{CV} - R_{CV}^0 e^{\Delta\tilde{\mu}_{CV}} \right) + \left(G_{IC} - R_{IC}^0 e^{\Delta\tilde{\mu}_{IC}} \right) \quad (22)$$

Owing to Kirchhoff laws eq. (4) and (5), it is possible to estimate the recombination rate from conduction to intermediate band

$$R_{IC}^0 e^{\Delta\tilde{\mu}_{IC}} = \frac{G_{IC} - G_{IV} + \sqrt{(G_{IC} - G_{IV})^2 + 4R_{IV}^0 R_{IC}^0 e^{\Delta\tilde{\mu}_{CV}}}}{2} \quad (23)$$

and the current can be expressed as a function of the applied bias only:

$$\frac{J}{q} = \left(G_{CV} - R_{CV}^0 e^{qV/kT_C} \right) + \left(\frac{G_{IV} + G_{IC}}{2} - \sqrt{\left(\frac{G_{IV} + G_{IC}}{2} \right)^2 + R_{IV}^0 R_{IC}^0 \left(e^{qV/kT_C} - \frac{G_{IV} G_{IC}}{R_{IV}^0 R_{IC}^0} \right)} \right) \quad (24)$$

From this expression, it is straightforward to show that, for the open circuit voltage V_{OC} to match that of the corresponding single junction $V_{OC}^{(1)} = \frac{kT_C}{q} \log \left(\frac{G_{CV}}{R_{CV}^0} \right)$, generation and recombination rates must verify

$$\frac{G_{IV} G_{IC}}{R_{IV}^0 R_{IC}^0} = \frac{G_{CV}}{R_{CV}^0} \quad (25)$$

hence eq.(21). Furthermore, provided that IC and IV recombinations are low enough, as is the case thanks to the ratchet energy shift, we consider $\left(\frac{G_{IV} + G_{IC}}{2} \right)^2 \gg R_{IV}^0 R_{IC}^0 \left(e^{qV/kT} - \frac{G_{IV} G_{IC}}{R_{IV}^0 R_{IC}^0} \right)$ and the previous expression can be simplified to

$$\frac{J}{q} \simeq \left(G_{CV} + \frac{G_{IV} G_{IC}}{G_{IV} + G_{IC}} - e^{qV/kT_C} \left(R_{CV}^0 + \frac{R_{IV}^0 R_{IC}^0}{G_{IV} + G_{IC}} \right) \right) \quad (26)$$

It is straightforward to estimate the open circuit voltage V_{OC} by setting $J = 0$

$$e^{qV_{OC}/kT_C} = \left(G_{CV} + \frac{G_{IV} G_{IC}}{G_{IV} + G_{IC}} \right) / \left(R_{CV}^0 + \frac{R_{IV}^0 R_{IC}^0}{G_{IV} + G_{IC}} \right) \quad (27)$$

The maximal power point V_m is defined by $\partial_V J \times V|_{V=V_m} = 0$, leading to

$$0 = G_{CV} + \frac{G_{IV} G_{IC}}{G_{IV} + G_{IC}} - \left(R_{CV}^0 + \frac{R_{IV}^0 R_{IC}^0}{G_{IV} + G_{IC}} \right) \left(1 + \frac{qV_m}{k_B T} \right) e^{qV_m/kT_C} \quad (28)$$

and the prefactor can be recognized from eq. (27), resulting in the same relation between V_{OC} and V_m as in a single junction

$$\left(1 + \frac{qV_m}{kT} \right) \exp \left(\frac{qV_m}{kT_C} \right) = \exp \left(\frac{qV_{OC}}{kT_C} \right) \quad (29)$$

hence eq.(17).

Lagrange multipliers

In this section, we derive results presented in the main text based on Lagrange multiplier approach. This approach consists in treating all parameters as free parameters, and accounting for constraints through additional terms included in the Lagrangian (12). The optimum configuration respecting these constraints is

reached when the derivative of L_R with respect to all parameters and multipliers is zero. It is straightforward to show that Kirchhoff's laws eq.(4-5) are recovered from the derivative of the Lagrangian with respect to the Lagrange multipliers λ_V and λ_I respectively.

Let us first consider the derivative of L_R with respect to E_{gIC} and E_{gIV} respectively.

$$\partial_{E_{gIC}} L_R = 0 \Rightarrow \Delta\mu_{IC} = qV_{gm,IC} \text{ or } \Delta\mu_{IC} = \lambda_I \quad (30)$$

$$\partial_{E_{gIV}} L_R = 0 \Rightarrow \Delta\mu_{IV} = qV_{gm,IV} \text{ or } \Delta\mu_{IV} = -\lambda_I \quad (31)$$

These relations result in four options, which we will now examine.

Option 1 $\Delta\mu_{IC} = \lambda_I$ and $\Delta\mu_{IV} = -\lambda_I$

In this case, following Kirchhoff's voltage law eq.(4), we find that the maximum power point is $qV_m = \Delta\mu_{CV} = 0$, which is absurd.

To discriminate between the three remaining options, we consider derivatives of the Lagrangian with respect to the quasi-Fermi levels splitting $\Delta\mu_{IC}$ and $\Delta\mu_{IV}$, together with Kirchhoff's current law eq.(5), leading to:

$$(\Delta\mu_{IV} + \lambda_I) R_{IV}^0 e^{\Delta\tilde{\mu}_{IV}} = (\Delta\mu_{IC} - \lambda_I) R_{IC}^0 e^{\Delta\tilde{\mu}_{IC}} \quad (32)$$

Option 2 $\Delta\mu_{IC} = \lambda_I$ and $\Delta\mu_{IV} = qV_{gm,IV}$

In this case, the right hand side is zero, leading to $qV_{gm,IV} = \Delta\mu_{IV} = -\lambda_I$ and we are back to option 1.

Option 3 $\Delta\mu_{IC} = qV_{gm,IC}$ and $\Delta\mu_{IV} = -\lambda_I$

In this case, the left hand side is zero, leading to $qV_{gm,IC} = \Delta\mu_{IC} = \lambda_I$ and we are back to option 1.

Option 4 $\Delta\mu_{IC} = qV_{gm,IC}$ and $\Delta\mu_{IV} = qV_{gm,IV}$

We are left with only this option, and will consider in the following

$$\Delta\mu_{IC} = qV_{gm,IC} \quad (33)$$

$$\Delta\mu_{IV} = qV_{gm,IV} \quad (34)$$

These expressions can be used to estimate the expression of the Lagrange multiplier:

$$\lambda_I = \frac{\Delta\mu_{IC} R_{IC}^0 \exp\left(\frac{\Delta\mu_{IC}}{kT_C}\right) - \Delta\mu_{IV} R_{IV}^0 \exp\left(\frac{\Delta\mu_{IV}}{kT_C}\right)}{R_{IV}^0 \exp\left(\frac{\Delta\mu_{IV}}{kT_C}\right) + R_{IC}^0 \exp\left(\frac{\Delta\mu_{IC}}{kT_C}\right)} \quad (35)$$

which in turn can be used to develop $\partial_{E_{gCV}} L_R = 0$ as

$$\exp\left(\frac{qV_m}{kT_C}\right) \left(1 + \frac{R_{IC}^0 \exp\left(\frac{\Delta\mu_{IC}}{kT_C}\right) - 1}{R_{IV}^0 \exp\left(\frac{\Delta\mu_{IV}}{kT_C}\right)}\right) = \frac{\partial_{E_{gCV}} G_{CV}}{\partial_{E_{gCV}} R_{CV}} \quad (36)$$

hence eq.(14).